Proceedings of the Sixteenth International Conference on
Computational Structures Technology
Edited by: P. Iványi, J. Kruis and B.H.V. Topping
Civil-Comp Conferences, Volume 14, Paper 13.1
Civil-Comp Press, Edinburgh, United Kingdom, 2026
ISSN: 2753-3239, doi: 10.4203/ccc.14.13.1

Application of Optimized Seismic Meta-Blocks to Reduce Ground Vibration

M. N. A. Nguyen, M. P. Truong, V. H. Nguyen and J. H. Lee

Department of Ocean Engineering, Pukyong National University Busan, South Korea

Abstract

Seismic metamaterials have attracted increasing attention as an effective alternative to conventional vibration mitigation techniques due to their ability to attenuate elastic waves through the formation of frequency band gaps. However, the design and optimisation of three-dimensional seismic metamaterials that simultaneously consider band-gap performance and construction cost remain insufficiently explored. In order to address this gap, this study proposes a systematic multi-objective optimisation framework for the design of seismic metamaterial structures, accounting for both targeted band-gap characteristics and material usage efficiency. Numerical models have been developed to evaluate the vibration attenuation performance of the optimised configurations in the frequency domain. The present study investigates the effects of key system parameters, including the number of meta-block columns and layers, in order to elucidate their influence on wave attenuation behaviour. The findings indicate that the optimised metamaterial configurations attain substantial reductions in ground vibration in comparison with the reference case, while concurrently preserving practical feasibility. The proposed optimization framework provides a flexible and effective approach for three-dimensional metamaterial design and shows strong potential for applications in structural vibration control and seismic protection engineering.

Keywords: seismic metamaterial, periodic structure, frequency band gap, optimization technique, meta-barrier, vibration mitigation.

1 Introduction

Ground-borne vibrations generated by seismic activity [1], transportation systems [2, 3], and industrial operations [4, 5] represent a persistent challenge in structural and geotechnical engineering, particularly for infrastructure requiring high serviceability and long-term durability . In the absence of adequate control measures, such vibrations have the potential to induce excessive deformation, accelerate material degradation, and ultimately compromise the structural integrity of the structure [6-8]. Whilst traditional vibration mitigation methods such as open or filled trenches, cylindrical piles, base isolations are efficacious in certain applications, they frequently necessitate the incorporation of additional damping or substantial isolation systems, which can be challenging to calibrate, expensive to install, and constrained in their capacity to target specific frequency ranges.

In this context, seismic metamaterials [9-11] have emerged as a promising alternative due to their ability to regulate elastic wave propagation through engineered periodicity, leading to the formation of frequency band gaps (FBGs). The exploitation of structural configuration as opposed to energy dissipation enables passive, frequency-selective vibration attenuation. This offers new possibilities for broadband control through rational design. Depending on the strategy of implementation, seismic metamaterials are commonly classified as seismic soil metamaterials [12], above-surface resonators [13], auxetic materials [14], or buried mass resonators [15]. While each category exhibits distinct advantages, they are also subject to significant practical limitations. Soil-based metamaterials necessitate substantial ground modification and are challenging to implement for deep-wave mitigation, whereas above-surface resonators require significant spatial requirements and are susceptible to environmental influences. Auxetic metamaterials have been demonstrated to exhibit distinctive wave attenuation capabilities; however, challenges related to manufacturing complexity, durability, and integration with existing structures persist. Conversely, buried mass resonators offer a compact and adaptable subterranean solution, with enhanced tunability through geometric and material parameters. However, many extant designs rely on oversized structures [9], or high damping levels [16], resulting in increased cost and limited scalability.

In this regard, the present study proposes a multi-objective optimisation framework for the three-dimensional (3D) design of seismic metamaterials with controlled band-gap properties. The proposed approach integrates parametric modelling, numerical simulation, and evolutionary optimisation algorithms to simultaneously maximise vibration attenuation and minimise material consumption. A series of numerical investigations are conducted with the aim of evaluating the vibration mitigation performance of the optimised configurations. Furthermore, the influence of key system parameters such as number of columns and number of layers on ground-borne wave suppression is examined. The findings demonstrate that the proposed framework provides an effective and flexible strategy for the practical optimisation of seismic metamaterials, with significant potential for applications in vibration mitigation and seismic protection engineering.

2 Methods

2.1 Periodic theory

The governing equation of wave propagation in elastic medium can be expressed as follow:

$$\mu\nabla^2\boldsymbol{u}(\boldsymbol{r},t) + (\lambda+\mu)\nabla\nabla\cdot\boldsymbol{u}(\boldsymbol{r},t) = \rho\frac{\partial^2\boldsymbol{u}(\boldsymbol{r},t)}{\partial t^2} \tag{1}$$

where $\boldsymbol{u}(\boldsymbol{r},t)$ is the displacement vector of the periodic medium, and $\lambda(\boldsymbol{r})$ and $\mu(\boldsymbol{r})$ are Lame's constants of the medium, $\rho(\boldsymbol{r})$ is the mass density of the medium, $\boldsymbol{r} = (x,y,z)$ is the position vector, ∇ is the gradient operator, and t is time. The arrangement of the periodic meta-barrier structure creates a Floquet-Bloch nature. According to the Floquet-Bloch theory [17], the solution from Equation (1) can be expressed as follow:

$$\boldsymbol{u}(\boldsymbol{r},t) = e^{i(\boldsymbol{k}\cdot\boldsymbol{r}-\omega t)}\boldsymbol{u_k}(\boldsymbol{r}) \tag{2}$$

where $\boldsymbol{u_k}(\boldsymbol{r})$ is the displacement modulation function that represents displacement amplitude for the corresponding Bloch wavevector $\boldsymbol{k}$, ω is the angular frequency, and i is the imaginary unit.

To satisfy the periodicity, the displacement vector $\boldsymbol{u_k}(\boldsymbol{r}+\boldsymbol{a})$, where $\boldsymbol{a} = n_1\boldsymbol{a}_1 + n_2\boldsymbol{a}_2 + n_3\boldsymbol{a}_3$ is the lattice constant vector and $\boldsymbol{a}_1$, $\boldsymbol{a}_2$, and $\boldsymbol{a}_3$ are primitive vectors of the Bravais lattice, must have the same amplitude as $\boldsymbol{u_k}(\boldsymbol{r})$:

$$\boldsymbol{u_k}(\boldsymbol{r}) = \boldsymbol{u_k}(\boldsymbol{r}+\boldsymbol{a}) \tag{3}$$

The periodic boundary condition (PBC) can be obtained when substitute Equation (3) into Equation (1):

$$\begin{aligned}\boldsymbol{u_k}(\boldsymbol{r}+\boldsymbol{a},t) &= \boldsymbol{u_k}(\boldsymbol{r}+\boldsymbol{a})e^{i(\boldsymbol{k}(\boldsymbol{r}+\boldsymbol{a})-\omega t)} \\ &= e^{i\boldsymbol{k}\cdot\boldsymbol{a}}\boldsymbol{u_k}(\boldsymbol{r})e^{i(\boldsymbol{kr}-\omega t)} = e^{i\boldsymbol{k}\cdot\boldsymbol{a}}\boldsymbol{u}(\boldsymbol{r},t)\end{aligned} \tag{4}$$

The dispersion equation can be transferred into eigenvalue problem when combining Equation (1) and Equation (4):

$$(\boldsymbol{K}(\boldsymbol{k}) - \omega^2\boldsymbol{M})\boldsymbol{u} = 0 \tag{5}$$

where $\boldsymbol{K}(\boldsymbol{k})$ is the stiffness matrix and $\boldsymbol{M}$ is the mass matrix of a unit cell. The dispersion curves can be obtained by sweeping the wavevector $\boldsymbol{k}$ along the boundaries $\mathrm{R}-\mathrm{M}-\Gamma-\mathrm{X}-\mathrm{M}$ in the first irreducible Brillouin zone using COMSOL Multiphysics [18]. Consequently, FBG can be obtained based on the dispersion curves.

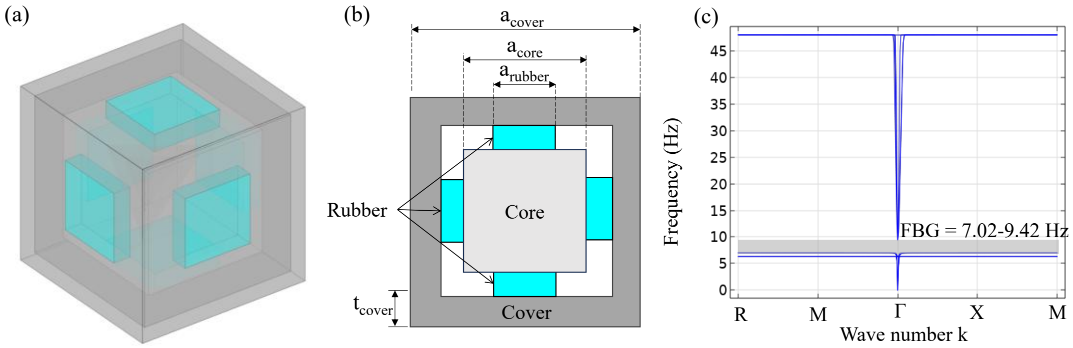

Figure 1: Configuration and properties of the proposed seismic metamaterial: (a) 3D configuration; (b) Vertical section; (c) FBG determination of an example meta-block.

Material	Density [kg/m^3]	Young's modulus [MPa]	Poisson's ratio [-]
Concrete	2400	3000	0.25
Rubber	0.6	0.6	0.47

Table 1: Meta-block material properties.

The configuration of a typical unit cell calling meta-block is displayed in Figure 1(a) and (b). The cover and the core of the unit cell are assigned with concrete, and the material connecting the cover with the core is defined as rubber. The material properties of the unit cell components are enumerated in Table 1. For a unit cell with $a_{cover} = 1\ (m)$, $t_{cover} = 0.05\ (m)$, $a_{core} = 0.6\ (m)$, $a_{rubber} = 0.25\ (m)$, the FBG (grey zone) is defined as the frequency range between $f_{min}^{FBG} = 7.02\ (Hz)$ and $f_{max}^{FBG} = 9.42\ (Hz)$, as determined by the acquisition of the dispersion curves (blue lines). The results displayed in Figure 1(c) showing that waves travelling within this frequency range cannot transmit through the unit cell.

2.2 Optimization procedure

In this study, a multi-objective optimisation framework is developed to determine the optimal configuration of the seismic metamaterial unit cell. The two objectives under consideration are as follows: (i) maximization of the targeted frequency band-gap (FBG) performance, and (ii) minimization of material usage to ensure practical construction feasibility. Five key design variables are selected for optimization, including the geometric dimensions and material properties of the meta-block components.

Appropriate parameter bounds and practical constraints are imposed to ensure realistic and constructible designs. The present study investigates several representative target FBG ranges in order to examine the relationship between the optimized parameters and the desired band-gap characteristics. The optimization process is performed using a genetic algorithm implemented in MATLAB, and the Pareto front of optimal solutions is obtained under the defined constraints.

The influence of individual design parameters on the FBG limits is evaluated through parametric studies and nonlinear regression analysis. The findings indicate that the cover size and core mass are the most significant factors determining the achievable FBG range, while variations in rubber stiffness demonstrate comparatively minor effects. It is evident from the observations that empirical relationships can be derived in order to establish a link between the optimal design parameters and the target FBG characteristics. This facilitates the rapid estimation of unit-cell configurations without the necessity of repeated optimisation.

Figure 2 presents the relationships between the optimised parameters and the corresponding FBG limits, while Figure 3 illustrates the regression-based trends used to express the optimal design variables as functions of the desired FBG. The findings indicate that the proposed optimisation approach offers an effective and systematic methodology for designing seismic metamaterials that are tailored to specific vibration isolation requirements.

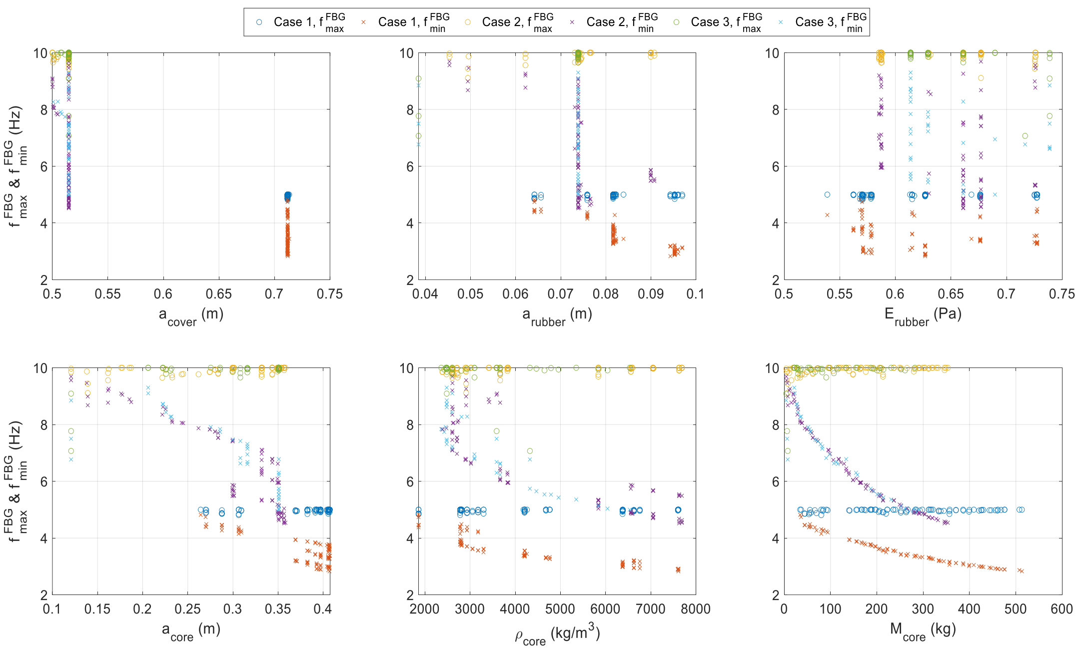

Figure 2: Relationship between the optimized parameters with f_{max}^{FBG} and f_{min}^{FBG}.

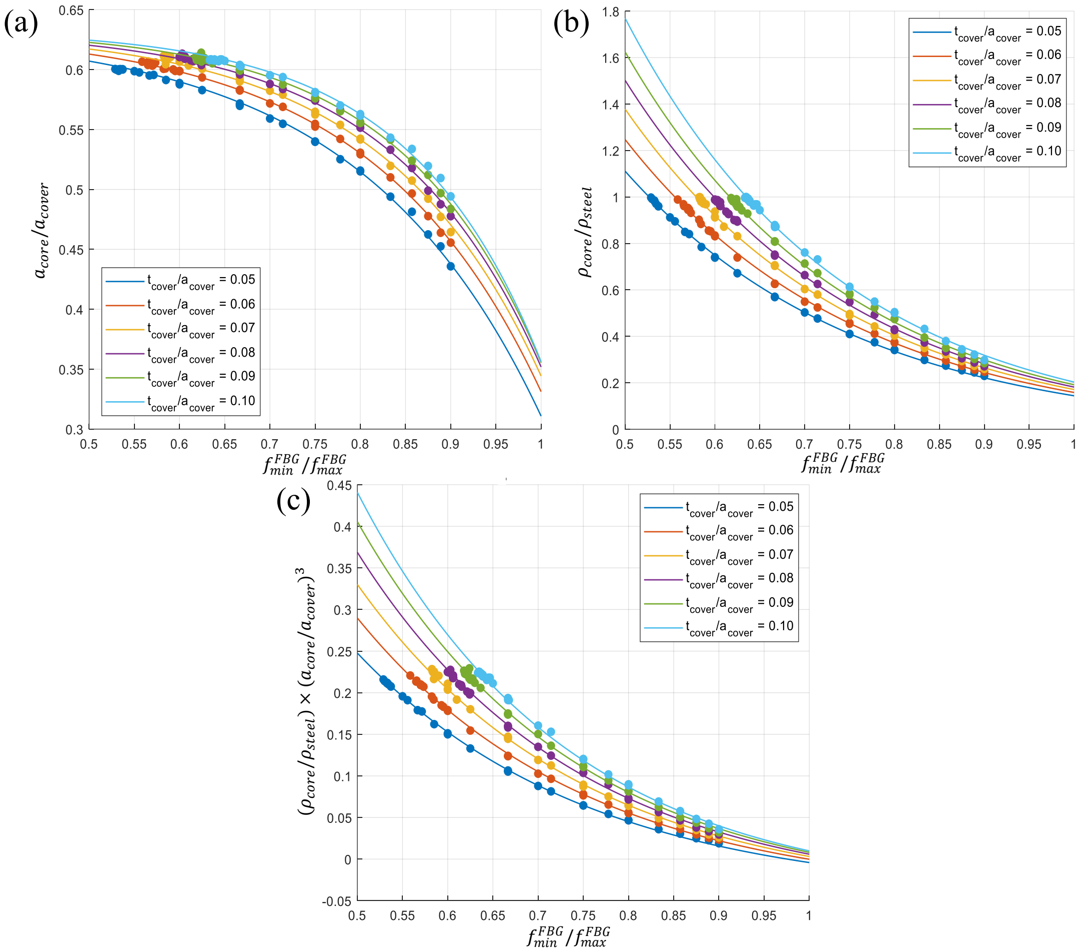

Figure 3: Nonlinear regression for parameters of the unit cell.

3 Application of the optimized meta-block

3.1 Numerical model

The vibration attenuation performance of the optimized meta-block is evaluated through numerical simulation within a representative soil domain. A 3D finite-element model is developed in COMSOL Multiphysics to simulate the propagation of elastic waves in soil with an embedded meta-block system (meta-barrier). The soil medium is modelled as a homogeneous elastic continuum with material properties defined as follows: density ρ_{soil} = 2000 kg/m^3, Young's modulus E_{soil} = 54 MPa, Poisson's ratio μ = 0.35, and shear wave velocity V_s = 100 m/s. Based on these parameters, the Rayleigh wave velocity is calculated to be V_R = 93.4 m/s. For the selected target frequency of 3 Hz, the corresponding Rayleigh wavelength is determined as λ_R = 31.13 m is selected. Appropriate boundary conditions are applied to ensure accurate wave propagation within the model. Roller boundary conditions are imposed on the left side of the domain, while periodic boundary conditions are assigned to the front and back planes to represent an infinite extent in the transverse direction. To suppress artificial reflections from model boundaries, perfectly matched layers (PMLs) with a thickness of $\lambda_R/2$ are implemented along the right side and bottom of the domain. The out-of-plane thickness of the model is defined as a_{cover} and additional geometric parameters are illustrated in Figure 4. Excitation is introduced in the form of a harmonic vertical displacement with unit amplitude $u_z = 1\ m$ applied along an edge line on the right side of the model. The SMS is positioned at a distance of $2\lambda_R$ from the excitation source. To quantify the vibration isolation performance, a monitoring region with area $S = a_{cover} \cdot \lambda_R$ is defined downstream of the meta-barrier. The attenuation efficiency is evaluated using a transfer function (TF), expressed as:

$$TF = 20log_{10}\frac{\overline{Z_1}}{\overline{Z_0}}(dB) \tag{10}$$

where $\overline{Z_0}$ and $\overline{Z_1}$ represent the average vertical displacement amplitude over the surface S in case of without SMS and with SMS, respectively.

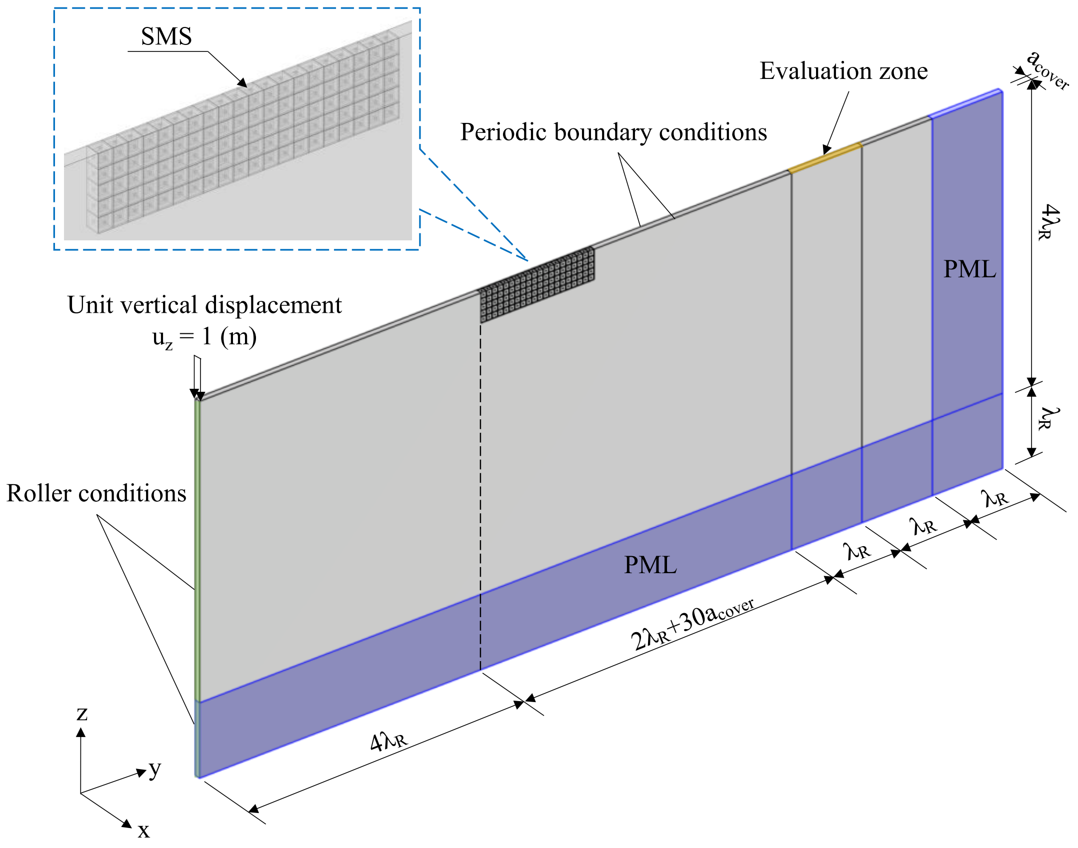

Figure 4: 3D numerical model with embed meta-block system.

3.2 Results

As demonstrated in Figure 5, the proposed meta-barrier generates a clear frequency band gap between 3–5.66 Hz, resulting in effective attenuation of ground-borne vibrations. The incorporation of the meta-barrier results in a reduction of peak amplitudes within the target band by more than 50%. The transfer-function spectra provide further confirmation of this trend, with attenuation levels exceeding 15–20 dB. The augmentation of columns has been demonstrated to enhance performance by extending the interaction length and enhancing cumulative scattering. However, the benefit appears to saturate at approximately 25 columns. Conversely, increasing the number of layers offers only marginal enhancement due to predominantly horizontal wave propagation, while concurrently escalating construction cost and complexity (Figure 6). Localised amplification has been observed in small arrays, and this phenomenon has been attributed to finite-size resonance effects. However, these effects are effectively suppressed in larger configurations. The results obtained demonstrate that the meta-barrier provides selective and efficient vibration mitigation within the designed band gap.

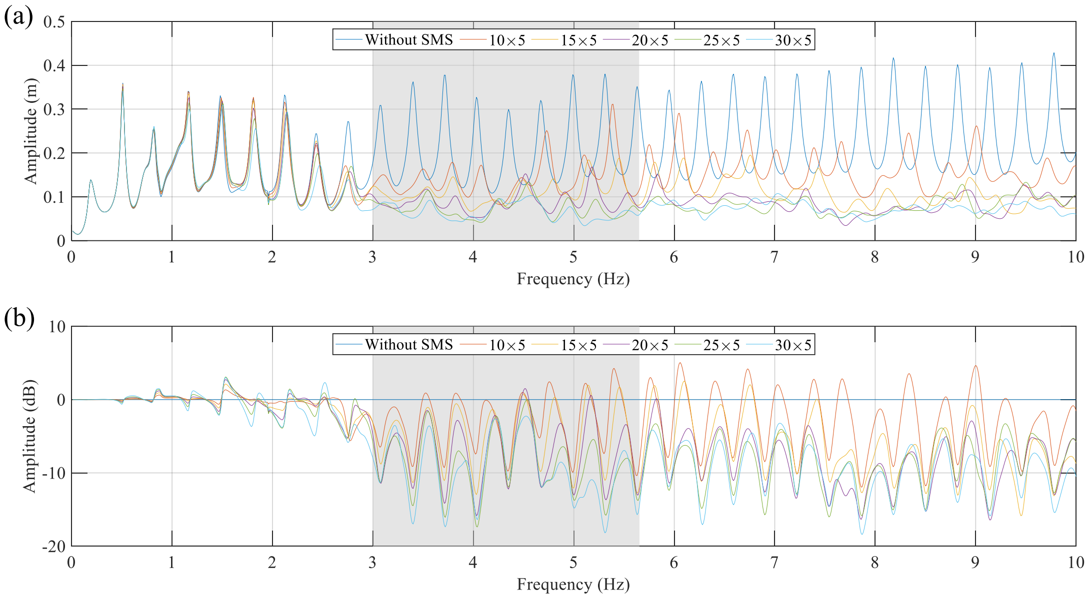

Figure 5: Effects of increasing number of columns of meta-block: (a) Vertical displacement amplitude; (b) Transfer function.

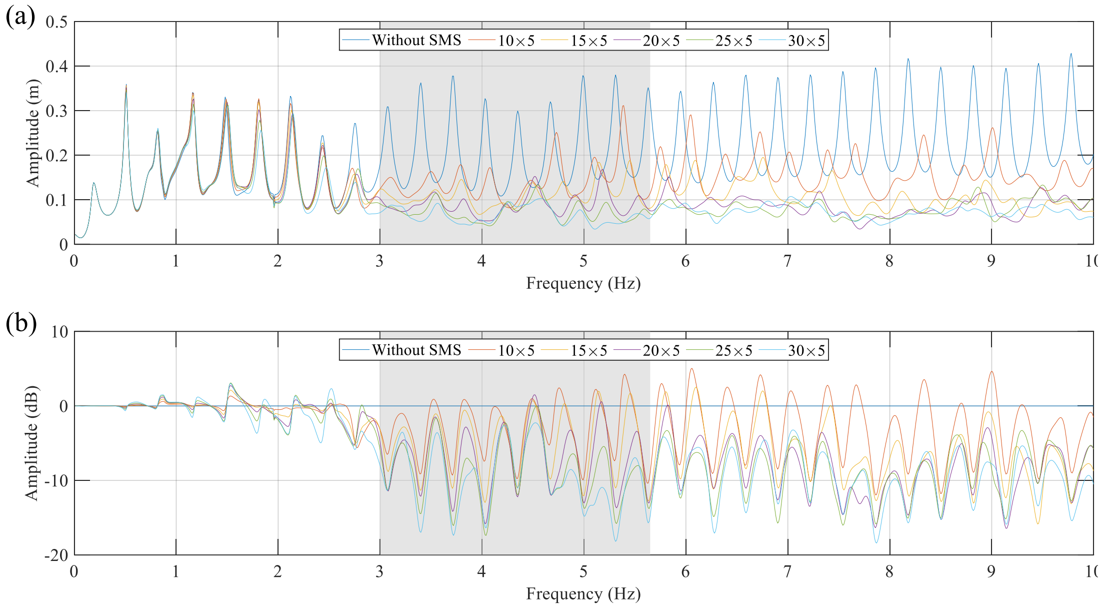

Figure 6: Effects of increasing number of layers of meta-block: (a) Vertical displacement amplitude; (b) Transfer function.

As illustrated in Figure 7, the vertical displacement contours are presented at varying excitation frequencies, thereby demonstrating the contrasting wave-propagation behaviour observed between the reference model and the meta-barrier configurations (30×5 and 5×30). In the absence of the meta-barrier, surface waves propagate with minimal distortion and no attenuation within the 3–5.66 Hz band-gap range. Conversely, both configurations manifest evident vibration suppression within this frequency range, as wave energy becomes concentrated near the source or dispersed within the meta-block array, leading to diminished transmission. Attenuation demonstrates marked frequency dependence, exhibiting limited efficacy at low frequencies (1–2 Hz) due to wavelengths exceeding the structural dimensions. Conversely, within the band gap, the synergistic effect of local resonance and periodic scattering gives rise to destructive interference and substantial suppression. The 30×5 configuration has been demonstrated to achieve superior performance due to its longer horizontal interaction length, which has been shown to enhance cumulative scattering and phase mismatch. The findings suggest that the efficacy of the proposed meta-barrier can be customised through geometric configuration. In scenarios where horizontal space is constrained, augmenting the number of vertical layers presents a pragmatic, albeit cost-dependent, solution for achieving attenuation within the designated band gap.

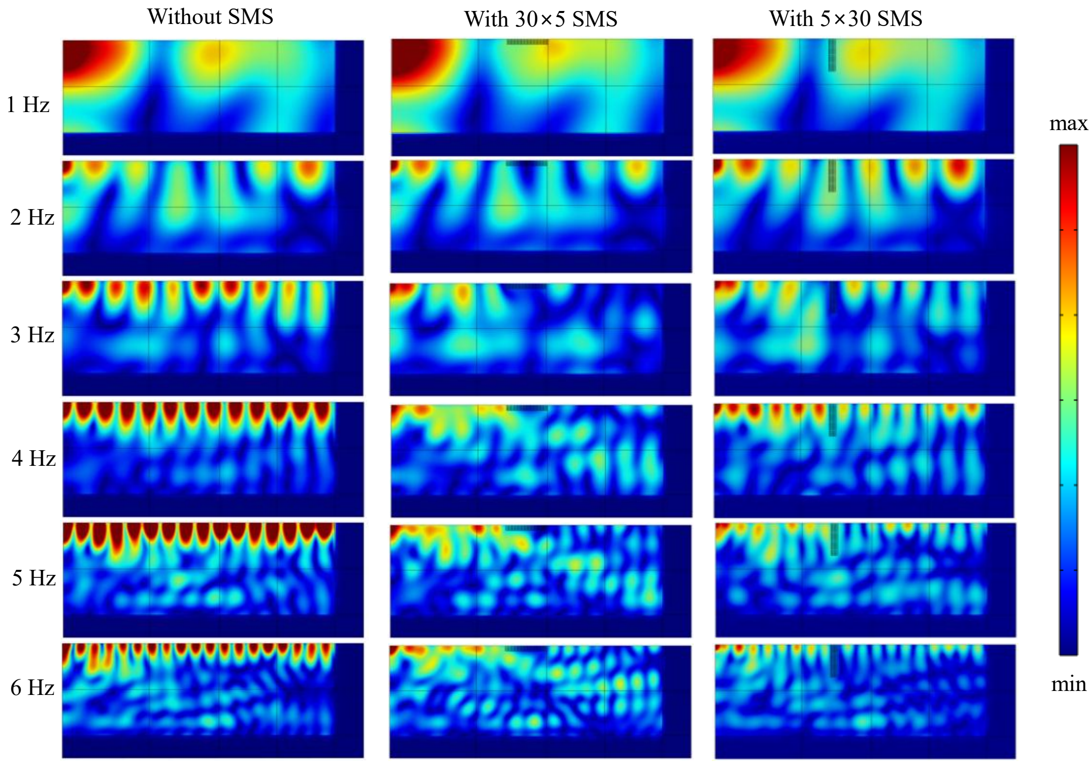

Figure 7: Contour of vertical displacement in different cases.

4 Conclusions and Contributions

A systematic multi-objective optimisation framework for the design of 3D seismic metamaterials has been developed, enabling simultaneous consideration of frequency band-gap performance and material usage efficiency. The proposed approach integrates parametric modelling, numerical simulation, and evolutionary optimisation to determine optimal meta-block configurations that achieve effective vibration attenuation with practical construction cost. The optimisation strategy successfully identifies structural layouts that maximise attenuation within target frequency ranges while minimising material consumption. The optimised designs demonstrate clear improvements in band-gap characteristics and enhanced vibration mitigation compared with non-optimised configurations.

The metamaterial configurations obtained in this study have been optimised for practical engineering implementation, with the potential to provide cost-effective and constructible solutions for ground vibration control. The findings of the present study demonstrate that a rational adjustment of key geometric parameters, such as the number of columns and layers, enables tailored performance without excessive material use. These findings underscore the viability of leveraging optimization-driven design in the context of seismic metamaterials for the purpose of safeguarding real-world infrastructure. Subsequent endeavours will centre on the augmentation of the framework to encompass larger-scale and more intricate soil–structure interaction problems, the enhancement of computational efficiency, and the exploration of a more extensive range of applications in seismic isolation and vibration mitigation systems. The proposed methodology offers a promising pathway towards the practical and intelligent design of next-generation seismic metamaterials.

Acknowledgements

This research was supported by the project “Development of Construction Technologies for Safe and Convenient Underground Roads (K-SCOUR)”, conducted under the Institution-led Strategic Development (ISD) program at the Korea Institute of Civil Engineering and Building Technology (KICT).

References

[1] J. F. Bird and J. J. Bommer, "Earthquake losses due to ground failure," *Engineering geology,* vol. 75, no. 2, pp. 147-179, 2004.
[2] H. Hao, T. Ang, J. J. B. Shen, and environment, "Building vibration to traffic-induced ground motion," vol. 36, no. 3, pp. 321-336, 2001.
[3] D. P. Connolly, G. P. Marecki, G. Kouroussis, I. Thalassinakis, and P. K. J. S. o. t. T. E. Woodward, "The growth of railway ground vibration problems—A review," vol. 568, pp. 1276-1282, 2016.
[4] B. M. J. T. New and u. s. technology, "Ground vibration caused by construction works," vol. 5, no. 3, pp. 179-190, 1990.
[5] G. Athanasopoulos, P. J. S. d. Pelekis, and e. engineering, "Ground vibrations from sheetpile driving in urban environment: measurements, analysis and effects on buildings and occupants," vol. 19, no. 5, pp. 371-387, 2000.
[6] P. Singh, M. J. I. J. o. R. M. Roy, and M. Sciences, "Damage to surface structures due to blast vibration," vol. 47, no. 6, pp. 949-961, 2010.
[7] M. J. B. S. Bata, "Effects on buildings of vibrations caused by traffic," vol. 6, no. 4, pp. 221-246, 1971.
[8] A. Papazoglou, A. J. E. E. Elnashai, and S. Dynamics, "Analytical and field evidence of the damaging effect of vertical earthquake ground motion," vol. 25, no. 10, pp. 1109-1137, 1996.
[9] M. Miniaci, A. Krushynska, F. Bosia, and N. M. Pugno, "Large scale mechanical metamaterials as seismic shields," *New Journal of Physics,* vol. 18, no. 8, p. 083041, 2016.
[10] C. Lim and J. Reddy, "Built-up structural steel sections as seismic metamaterials for surface wave attenuation with low frequency wide bandgap in layered soil medium," *Engineering Structures,* vol. 188, pp. 440-451, 2019.
[11] A. Colombi, D. Colquitt, P. Roux, S. Guenneau, and R. V. Craster, "A seismic metamaterial: The resonant metawedge," *Scientific reports,* vol. 6, no. 1, p. 27717, 2016.
[12] X. Pu and Z. Shi, "Surface-wave attenuation by periodic pile barriers in layered soils," *Construction and Building Materials,* vol. 180, pp. 177-187, 2018.

[13] Q. Du, Y. Zeng, Y. Xu, H. Yang, and Z. Zeng, "H-fractal seismic metamaterial with broadband low-frequency bandgaps," *Journal of Physics D: Applied Physics,* vol. 51, no. 10, p. 105104, 2018.
[14] X. Ren, R. Das, P. Tran, T. D. Ngo, and Y. M. Xie, "Auxetic metamaterials and structures: a review," *Smart Materials and Structures,* vol. 27, no. 2, p. 023001, 2018.
[15] A. Palermo, M. Vitali, and A. Marzani, "Metabarriers with multi-mass locally resonating units for broad band Rayleigh waves attenuation," *Soil Dynamics and Earthquake Engineering,* vol. 113, pp. 265-277, 2018.
[16] Y. Achaoui, B. Ungureanu, S. Enoch, S. Brûlé, and S. Guenneau, "Seismic waves damping with arrays of inertial resonators," *Extreme Mechanics Letters,* vol. 8, pp. 30-37, 2016.
[17] D. R. Hofstadter, "Energy levels and wave functions of Bloch electrons in rational and irrational magnetic fields," *Physical review B,* vol. 14, no. 6, p. 2239, 1976.
[18] C. J. C. M. Multiphysics, Burlington, MA, accessed Feb, "Introduction to comsol multiphysics®," vol. 9, no. 2018, p. 32, 1998.